OPTIMIZATION OF PHOTO-FISSION FRAGMENT PRODUCTION IN THE ELISOL SETUP AT ELI-NP

D. Nichita[1,2], P. Constantin[1], D.L. Balabanski[1,2], B. Mei[1], A. Rotaru[3], T. Sava[3], A. Spătaru[1,2], A. State[2,3], T. Dickel[4,5], B. Kindler[4], B. Lommel[4]

Within the ELI-NP (Extreme Light Infrastructure-Nuclear Physics) project developed in Magurele, Romania, an IGISOL (Ion Guided Isotope Separator On Line) facility is being designed in which exotic nuclei will be produced by the photo-fission of thin uranium foils then extracted and measured. The targets will be placed in a Cryogenic Stopping Cell (CSC) filled with He gas, in which the fission fragments will be thermalized and extracted, using both electric fields and gas flow. The optimization of the target system, aiming at maximizing the rate of ions released in the CSC gas, determining the optimum thickness, geometry and tilting angle of the targets and the optimum gamma beam energy range, is reported.

Keywords: ELISOL,ELI-NP,photo-fission,neutron rich ions,exotic nuclei

1. Introduction

Study of exotic nuclei in the neutron rich region of the nuclide chart stays in the central focus of contemporary nuclear physics. The main scientific motivation is the impact of such studies on areas like nuclear structure models, nuclear astrophysics, nuclear equation of state, etc.

A new major nuclear physics research infrastructure currently under construction in Europe is Extreme Light Infrastructure Nuclear-Physics (ELI-NP) [1]. The status of the implementation of ELI-NP and the emerging research

[1] Extreme Light Infrastructure – Nuclear Physics, "Horia Hulubei" National Institute for Physics and Nuclear Engineering, 30 Reactorului Street, 077125 Bucharest Magurele, Romania, dragos.nichita@eli-np.ro

[2] Doctoral School in Engineering and Applications of Lasers and Accelerators, University "Politehnica" of Bucharest, Romania

[3] "Horia Hulubei" National Institute for Physics and Nuclear Engineering, 30 Reactorului Street, 077125 Bucharest Magurele, Romania

[4] GSI Helmholtz Centre for Heavy Ion Research - Planckstrae 1, 64291 Darmstadt, Germany

[5] II. Physikalisches Institut, Justus-Liebig-Universit at Giessen, 35392 Giessen, Germany

program were reviewed recently [2]. Its main research instruments will be two 10 PW laser beams [3], and a high-brilliance gamma beam that will be produced through Compton Back Scattering of laser photons off highly energetic electrons accelerated with a linear particle accelerator [4].

This paper extends the study presented in Ref. [5] by using the actual target design and an improved parametrization of the photo-fission data. In addition, the experimental setup is optimized, taking into account several factors such as target thickness, number, geometry and tilting angle, as well as the gamma beam energy window in order to maximize the rate of fission fragments released in the gas of the CSC and minimize the rate of fragments that are stopped in the targets, backing, frame or in the rods supporting the target system.

2. **The ELISOL beamline at ELI-NP**

An IGISOL (Ion Guide Isotope Separator On-Line) facility is proposed at the ELI-NP gamma beam system (GBS) for the study of neutron rich nuclei [6] [7]. It uses the photo-fission reaction induced by exposing uranium targets to the high-brilliance $10^{12}\gamma/s$ gamma beam at ELI-NP in the energy range $10MeV - 19MeV$. The targets are placed in the center of the High Areal Density with Orthogonal extraction Cryogenic Stopping Cell (HADO-CSC), a concept introduced in Ref. [8]. The HADO-CSC consists of two chambers: production chamber and extraction chamber (Fig.1). To form a radioactive ion beam (RIB) from the fission fragments released with high kinetic energy, they need to be slowed down and extracted. To achieve this, the CSC is filled with low temperature He gas and the target system is placed inside it. The ions of the fission fragments will be slowed down in the gas and guided with both electric fields and gas flow to the extraction chamber. To avoid the loss of ions by hitting the cell walls, RF fields will be used. The RF Carpet will generate a strong repulsive electric field perpendicular to the wall. Fig. 1 shows the stages of fragment production, release and extraction. Downstream from the CSC, a Radio-Frequency Quadrupole (RFQ) will form the RIB to be sent to the measurement stations.

3. **Improved photo-fission model**

The extended parameterization $GIF^{238}U$ [9] of all available measurements of uranium photo-fission cross-sections and production yields has been implemented in the GEANT4 [10] modules described in Ref. [7]. This model covers a broad gamma energy interval from 0 to 30 MeV and reliably extends the description of the mass and charge yields into the heavy fragment region.

This improved parameterization was used to cross-check previous simulations [5] [7] which were based only on the photofission yield measurements in ultra-peripheral $^{238}U(\gamma^*, f)^{208}Pb$ collisions [11]. Experimental data are available for $Z \leq 52$, and an extrapolation was done for higher proton number.

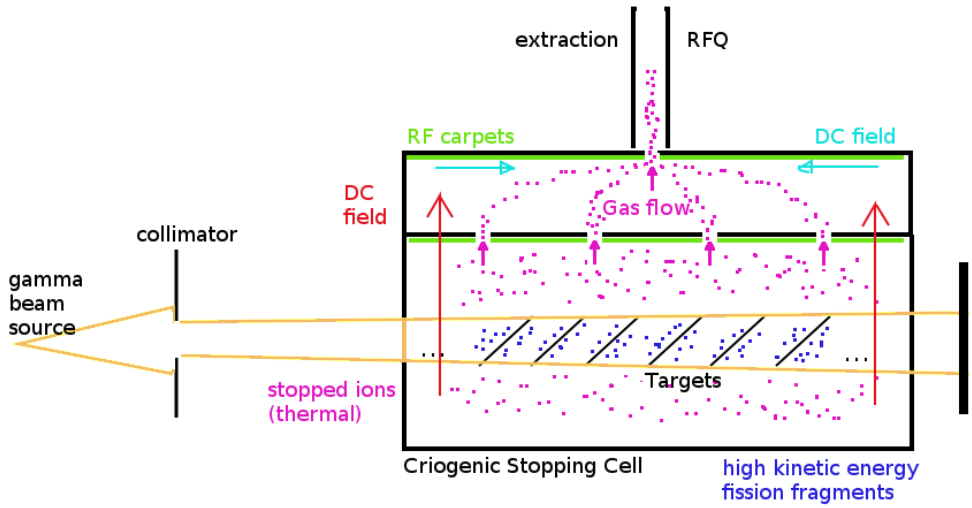

FIGURE 1. The motion of photo-fission fragments in the Cryogenic Stopping Cell (pink). The gamma beam (orange) is hitting the uranium compound targets (black) inside the CSC producing high kinetic energy photo-fission fragments (blue). The fragments are slowed down in the gas inside the lower chamber of the CSC becoming thermaized ions (pink) which are guided to the upper chamber using the vertical DC field (red) and the gas that flows upwards through the 4 nozzles. RF carpets (green) are used to repel the ions from the upper walls of the chambers. In the upper chamber a combination of horizontal DC fields (cyan), upward gas flow and RF fields (green) will help extract the ions.

More recent measurements [12] extend these data and, as described in Ref. [9], a strong deviation from a monotonic behavior develops in the heavy fragment region immediately after the cut off of the data set of Ref. [11].

Two GEANT4 classes were upgraded using the above parameterization, namely the classes for calculation of the total photo-fission cross-section and for the generation of the final state products of the photo-fission process.

The GEANT4 particle tracking algorithm involves the following steps: (1) the reaction cross-section is used to establish the type (probability) and location (mean free path) of a process; (2) if a photo-fission process happens, the outgoing photons and neutrons are generated according to the measured kinematic distributions at the current gamma beam energy; (3) the mass and charge yield distributions are used to identify the first fragment; (4) the identity of the second fragment is established based on mass and charge conservation; (5) the kinematic properties of both fragments are computed from energy and momentum conservation; (6) all final state particles are processed by the GEANT4 framework for further propagation.

The ratio between the isotopic yield distributions using the old and the new parameterizations, respectively, is shown in Fig. 2. A ratio around unity is obtained for all fragments, except the heaviest. Here, as expected from the new data presented in Fig. 3 of Ref. [9], the new parameterization generates higher yields but with low impact in overall results. Note that the lack of statistics in the tails of the isotope distributions leads to deviations from unity.

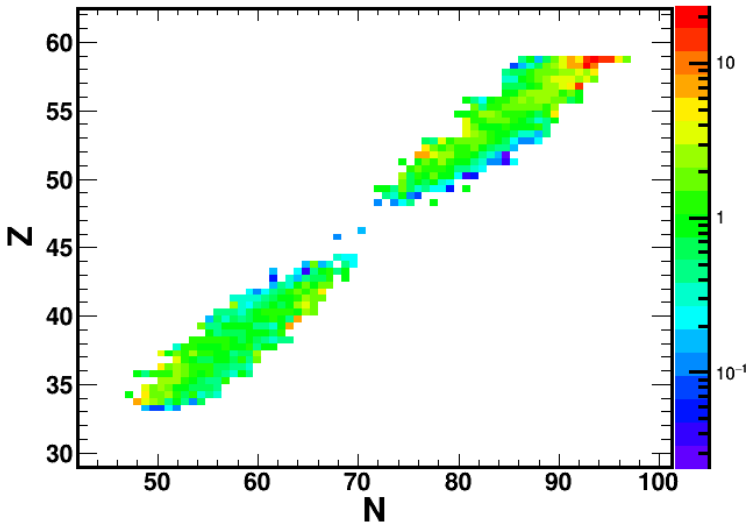

FIGURE 2. Ratio between the isotopic distributions obtained with the two parameterizations ($GIF^{238}U$ parametrization [9] vs. yield measurements from Ref. [11] polynomial fit function)

4. Design of the CSC target system

Previous work [5] [7] considered metallic uranium as target material. However, practical considerations related to mechanical and chemical properties of the targets, brought in consideration the use of various uranium compounds, such as uranium oxide UO_2, uranium carbide UC_2 and uranium tetrafluoride UF_4.

GEANT4 simulations have been performed for the three mentioned compounds and compared with the metallic uranium for different target thicknesses. The result of these calculations are presented in Fig. 3. An optimal areal density of 3 mg/cm^2 is obtained for all target materials.

In the present study we used uranium tetra-fluoride targets with a 3 μm optimal thickness embedded in 5 mm thick $AlMg_3$ target frames held together by four Fe rods, 3 mm in diameter. The targets have a 0.5 μm graphite backing.

The release rates, shown in Fig. 3, are obtained using a target system composed of 59 targets tilted at 10 degrees. At these rates the ion fraction stopped in all the target frames (about 15%), in the four rods (about 4%)

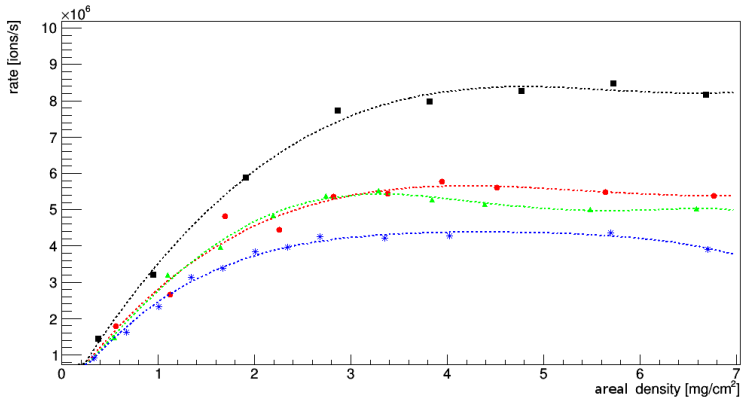

FIGURE 3. Yield of the released fragments as a function of the area density for the 3 uranium compounds UF_4 (blue stars), UC_2 (red circles), UO_2 (green triangles) and metallic uranium (black squares).

and in all the neighboring targets and graphite backings (less than 3%), were included.

The graphite layer has been used to increase the mechanical strength of the target foils. Beside manufacturing considerations, the percentage of the fragments stopped in this backing layer is the other factor considered in choosing the thickness t. This percentage is shown in Fig. 4 as a function of the graphite layer area density.

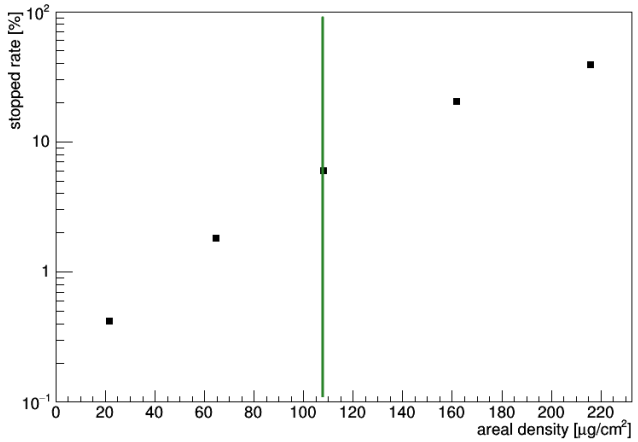

FIGURE 4. Percentage of the fragments entering the graphite backing stopped in this layer as a function of its areal density. The vertical green line corresponds to 0.5 μm graphite thickness chosen in our case.

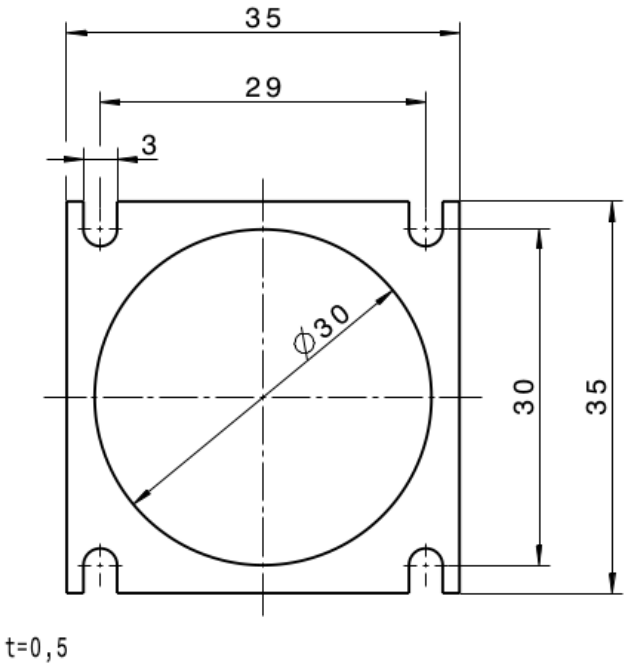

FIGURE 5. Design of the one target with its frame. Dimensions are given in millimeters.

The first set of six targets, intended for future online tests of the CSC demonstrator unit [13], was manufactured by the GSI target laboratory. They are made of uranium oxide UO_2 with a thickness of 2 μm (2.19 mg/cm^2 areal density) and are covered by a 0.5 μm thick graphite layer. This leads to a release rate of $8 \cdot 10^4$ $fragments/s$ from each target, out of which about 7% are lost in the backing. These targets come in an $AlMg_3$ rectangular frame whose drawing is shown in Fig. 5. The targets are circular with a diameter of 30 mm.

5. **Optimization of the CSC target system geometry**

In the full CSC device of the ELISOL facility at ELI-NP, a large number of such targets will be placed along the primary gamma beam. As described in Ref. [5], the geometry of this target system has several parameters that establish how the gamma beam spot is covered and how the available space inside the CSC is used optimally. We revisit here the optimization study, described in Ref. [5], and take in consideration the actual target and target frame design.

Circular targets, tilted with respect to the gamma beam, are seen as elliptical by the beam. Hence, it can not cover the cylindrically symmetric spot. Therefore, sets of two or three targets placed one on top of the other

have been considered creating target sets to better cover the primary beam spot.

The complete target system comprises sets of targets with their frames and the support structure formed by four steel rods and is shown in Fig. 6 for sets of one, two and three targets.

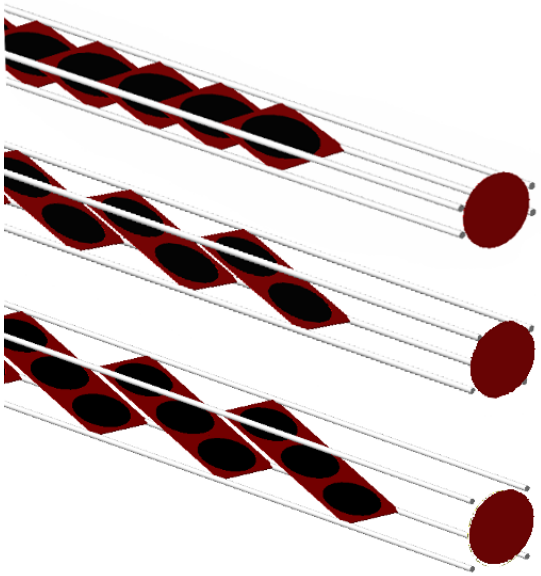

FIGURE 6. Target system with sets of one, two and three targets.

A complex optimization study of the target system geometry was performed in order to maximize the release rate of photo-fission fragments into the CSC gas. The main parameters of the optimization, and a description of their impact, are:

(1). The maximum energy of the gamma beam E_{γ}^{max} which is fixed by the energy of the accelerated electrons, as described in Ref. [5]. This sets the overlap between the beam intensity distribution and the photo-fission cross-section, as exemplified in Fig. 7. The gamma beam energy distribution is cut on the left side by the collimator due to the angle-energy correlation of the Compton back-scattering. The values used in the calculation are for $E_{\gamma}^{max} = 14, 14.5, 15, 16$ and $17 MeV$.

(2). The target tilting angle α with respect to the primary beam. Smaller values of the tilting angle increase the path length of the gammas inside the target foils, hence the fragment production rate, and also increase the available emission angle relative to the neighboring foils, as demonstrated in Fig. 8.

However, decreasing the tilting angle increases the longitudinal size of the target set and reduces the overall number of sets that can be placed inside the CSC. The values used in the calculations are tilted angles of 10 and 20 degrees.

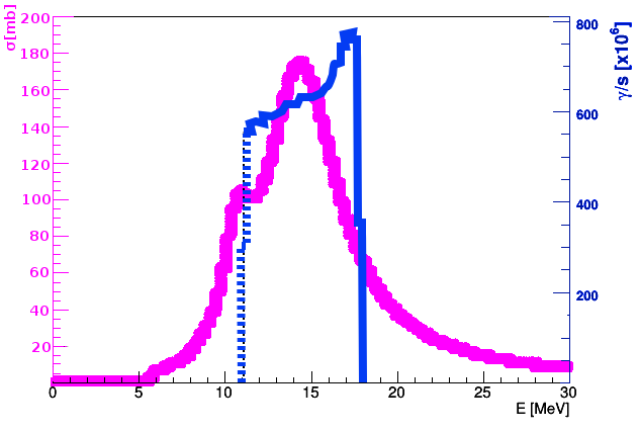

FIGURE 7. Gamma beam intensity distribution (blue line) overlapped with the photo-fission cross-section (pink line).

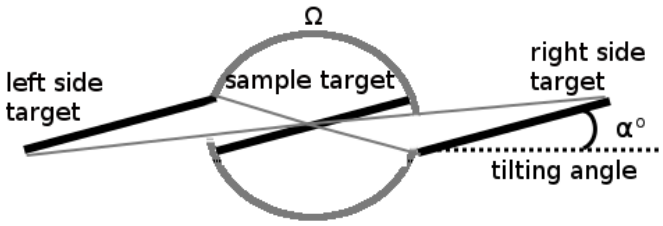

FIGURE 8. Targets with smaller tilting angles α have larger available emission angles Ω, relative to the neighboring targets, if the inter-target distance is the same.

(3). The number of targets per set which establish the coverage of the beam spot size. The largest dimension of the target on the orthogonal plane with respect to the beam axis fixes the beam spot size. However, due to the small tilting angle one dimension of the target is covering only a small fraction of the beam spot. Therefore, the increase of the number of targets per set gives a better coverage. This is demonstrated by the drawing in Fig. 9. The values used for calculations are one, two and three targets per set.

(4). The number of target sets which has impact on production rates. A larger number of targets is desired, however it is limited by the total length of the target system which was set to 2 m in these simulations.

6. **Results and Conclusions**

A large number of configurations have been simulated. In the simulations, in order to minimize the computational requirements, a number of 10^8 gamma rays has been generated for each configuration. These with the highest fragment release rates, within 2σ uncertainty, were selected for runs with

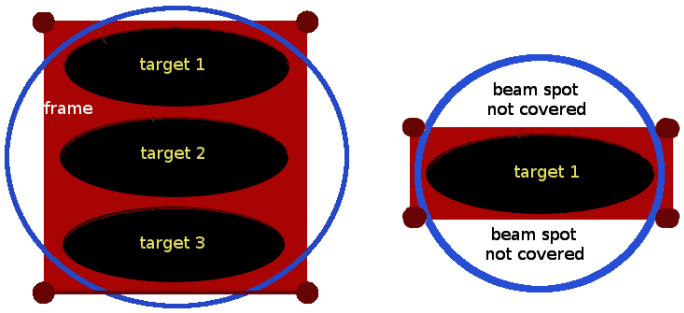

FIGURE 9. Example of difference in the beam spot size (blue circle) coverage ratio between three targets per set in the left image and one target per set in the right image.

increased statistics, more specifically with $4 \cdot 10^8$ gamma rays. The final five configurations are shown in Fig. 10 and give an estimated maximum rate of released and thermalized fragments of $3.5 \cdot 10^6$ ions/s, corresponding to the expected gamma beam rate of 10^{12} γ/s. The decision on which of these to be implemented will be made based upon criteria related to manufacturing and installation.

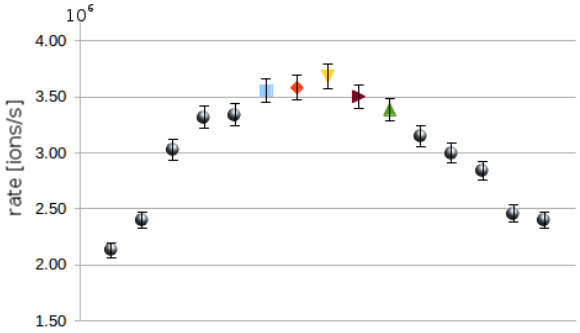

FIGURE 10. The five target system configurations with the highest ion release rate (with colored symbols) and the non-optimal configurations (gray circles). Each result shown corresponds to a specific system configuration. Three of the configurations have the same value of the gamma beam threshold energy $E_\gamma^{max} = 14.5\ MeV$: light blue for the results of 1 target/set tilted at 10 degrees, light red for the results of 2 targets/set tilted at 10 degrees, yellow for the results of 2 targets/set tilted at 20 degrees. The green triangle corresponds to the results of 3 targets/set tilted at 10 degrees configuration with $E_\gamma^{max} = 15\ MeV$. The dark red marker corresponds to the results of 3 targets/set tilted at 20 degrees configuration with $E_\gamma^{max} = 16\ MeV$.

In summary, after optimization, the ELISOL facility at ELI-NP is able to provide a significant rate of released ions available for experimental studies (above $3.5 \cdot 10^6$ ions/s). Thus, exotic nuclei with low production probability and short life-times can be measured and characterized for the first time or with higher accuracy than achieved so far.

7. ACKNOWLEDGEMENTS

The ELI-NP group was supported by Extreme Light Infrastructure Nuclear Physics (ELI-NP) Phase II, a project co-financed by the Romanian Government and the European Union through the European Regional Development Fund the Competitiveness Operational Programme (1/07.07.2016, COP, ID 1334). The IFIN-HH group was supported by the ELI-RO project financed by the Romanian Government through the Grant Programme ELI-RO-07.

The authors would like to acknowledge the support of Jutta Steiner and the whole group at the GSI target laboratory.

REFERENCES

[1] *N.V. Zamfir*, Extreme Light Infrastructure - Nuclear Physics (ELI-NP), Nuclear Physics News **25** (2015) 34

[2] *D.L. Balabanski et al.*, New light in nuclear physics: The Extreme Light Infrastructure Europhys. Lett. **117** (2017) 28001

[3] *D. Ursescu et al.*, Extreme light infrastructure nuclear physics (ELI-NP): present status and perspectives, Proc. SPIE **8780** (2013) 87801H-1

[4] *H.R. Weller et al.*, Gamma Beam Delivery and Diagnostic, Rom. Rep. Phys. **68** (2016) S447

[5] *P. Constantin et al.*, Design of the gas cell for the IGISOL facility at ELI-NP, Nucl. Instr. Meth. Phys. Res. B **397** (2017) 1-10

[6] *D.L. Balabanski et al.*, Photofission experiments at ELI-NP, Rom. Rep. in Phys. **68** (2016) S621

[7] *P.Constantin et al.*, Simulation of photofission experiments at the ELI-NP facility, Nucl. Instr. Meth. Phys. Res. B **372** (2016) 78-85

[8] *T. Dickel et al.*, Conceptional design of a novel next-generation cryogenic stopping cell for the Low-Energy Branch of the super-FRS, Nucl. Instr. Meth. Phys. Res. B **376** (2016) 216

[9] *B. Mei et al.*, Empirical parametrization for production cross sections of neutron-rich nuclei by photofission of ^{238}U at low energies, Phys. Rev. C **96** (2017) 064610

[10] *S. Agostinelli et al.*, GEANT4: A Simulation toolkit, Nucl. Instrum. Meth. Phys. Res. A **506** (2003) 250

[11] *C. Donzaud et al.*, Low-energy fission investigated in reactions of 750 AMeV U-ions on Pb. II: Isotopic distributions, Eur. Phys. J. A **1** (1998) 407

[12] *S. Pomme et al.*, Excitation energy dependence of charge odd-even effects in the fission of ^{238}U close to the fission barrier, Nucl. Phys. A **560** (1993) 689

[13] D.L. Balabanski et al., to appear in JPS Proceedings.